European Radiology (2019) 29:4957–4967
https://doi.org/10.1007/s00330-019-06066-2

NEURO

Relaxation-compensated amide proton transfer (APT) MRI signal intensity is associated with survival and progression in high-grade glioma patients

Daniel Paech[1] · Constantin Dreher[1] · Sebastian Regnery[1,2] · Jan-Eric Meissner[3] · Steffen Goerke[3] · Johannes Windschuh[3] · Johanna Oberhollenzer[1] · Miriam Schultheiss[1] · Katerina Deike-Hofmann[1] · Sebastian Bickelhaupt[1] · Alexander Radbruch[1,4] · Moritz Zaiss[5] · Andreas Unterberg[6] · Wolfgang Wick[7] · Martin Bendszus[8] · Peter Bachert[3] · Mark E. Ladd[3,9,10] · Heinz-Peter Schlemmer[1]

Received: 3 November 2018 / Revised: 28 December 2018 / Accepted: 4 February 2019 / Published online: 26 February 2019

Abstract

Objectives The purpose of this study was to investigate the association of relaxation-compensated chemical exchange saturation transfer (CEST) MRI with overall survival (OS) and progression-free survival (PFS) in newly diagnosed high-grade glioma (HGG) patients.

Methods Twenty-six patients with newly diagnosed high-grade glioma (WHO grades III–IV) were included in this prospective IRB-approved study. CEST MRI was performed on a 7.0-T whole-body scanner. Association of patient OS/PFS with relaxation-compensated CEST MRI (amide proton transfer (APT), relayed nuclear Overhauser effect (rNOE)/NOE, downfield-rNOE-suppressed APT (dns-APT)) and diffusion-weighted imaging (apparent diffusion coefficient) were assessed using the univariate Cox proportional hazards regression model. Hazard ratios (HRs) and corresponding 95% confidence intervals were calculated. Furthermore, OS/PFS association with clinical parameters (age, gender, O6-methylguanine-DNA methyltransferase (MGMT) promotor methylation status, and therapy: biopsy + radio-chemotherapy vs. debulking surgery + radio-chemotherapy) were tested accordingly.

Results Relaxation-compensated APT MRI was significantly correlated with patient OS (HR = 3.15, $p = 0.02$) and PFS (HR = 1.83, $p = 0.009$). The strongest association with PFS was found for the dns-APT metric (HR = 2.61, $p = 0.002$). These results still stand for the relaxation-compensated APT contrasts in a homogenous subcohort of $n = 22$ glioblastoma patients with isocitrate dehydrogenase (IDH) wild-type status. Among the tested clinical parameters, patient age (HR = 1.1, $p = 0.001$) and therapy (HR = 3.68, $p = 0.026$) were significant for OS; age additionally for PFS (HR = 1.04, $p = 0.048$).

Electronic supplementary material The online version of this article (https://doi.org/10.1007/s00330-019-06066-2) contains supplementary material, which is available to authorized users.

✉ Daniel Paech
d.paech@dkfz.de

[1] Division of Radiology, German Cancer Research Center (DKFZ), Im Neuenheimer Feld 280, 69120 Heidelberg, Germany

[2] Department of Radiation Oncology, University Hospital Heidelberg, Im Neuenheimer Feld 400, 69120 Heidelberg, Germany

[3] Division of Medical Physics in Radiology, German Cancer Research Center (DKFZ), Im Neuenheimer Feld 280, 69120 Heidelberg, Germany

[4] Department of Radiology, University Hospital Essen, Essen, Germany

[5] Magnetic Resonance Center, Max-Planck-Institute for Biological Cybernetics, Tuebingen, Germany

[6] Department of Neurosurgery, University Hospital Heidelberg, Im Neuenheimer Feld 400, 69120 Heidelberg, Germany

[7] Department of Neurology, University Hospital Heidelberg, Im Neuenheimer Feld 400, 69120 Heidelberg, Germany

[8] Department of Neuroradiology, University Hospital Heidelberg, Im Neuenheimer Feld 400, 69120 Heidelberg, Germany

[9] Faculty of Physics and Astronomy, University of Heidelberg, 69120 Heidelberg, Germany

[10] Faculty of Medicine, University of Heidelberg, 69120 Heidelberg, Germany

Conclusion Relaxation-compensated APT MRI signal intensity is associated with overall survival and progression-free survival in newly diagnosed, previously untreated glioma patients and may, therefore, help to customize treatment and response monitoring in the future.

Key Points

- *Amide proton transfer (APT) MRI signal intensity is associated with overall survival and progression in glioma patients.*
- *Relaxation compensation enhances the information value of APT MRI in tumors.*
- *Chemical exchange saturation transfer (CEST) MRI may serve as a non-invasive biomarker to predict prognosis and customize treatment.*

Keywords Magnetic resonance imaging · Glioma · Glioblastoma · Survival · Biomarkers, cancer

Abbreviations

APT	Amide proton transfer
APT_{AREX}	APT contrast calculated with the *AREX* metric
APT_{LD}	APT contrast calculated with the *LD* metric
AREX	Apparent exchange-dependent relaxation
CEST	Chemical exchange saturation transfer
dns-APT	Downfield relayed nuclear Overhauser effect suppressed APT
FLAIR	Fluid-attenuated inversion recovery
FoV	Field of view
GBCA	Gadolinium-based contrast agents
GBM	Glioblastoma multiforme
gdce-T1	T1-weighted gadolinium contrast-enhanced MRI
GRE	Gradient echo
HGG	High-grade glioma
IDH	Isocitrate dehydrogenase
IQR	Interquartile range
KPS	Karnofsky performance scale
LD	Lorentzian difference
MGMT	O6-Methylguanine-DNA methyltransferase
MITK	Medical Imaging Interaction Toolkit
MPRAGE	Magnetization-prepared rapid gradient echo
MTR_{asym}	Magnetization transfer ratio asymmetry
MTR_{LD}	Magnetization transfer Lorentzian difference
NOE	Nuclear Overhauser effect
NOE_{AREX}	NOE contrast calculated with the *AREX* metric
NOE_{LD}	NOE contrast calculated with the *LD* metric
OS	Overall survival
PFS	Progression-free survival
RANO	Response assessment in neuro-oncology
rCBV	Relative cerebral blood volume
RCT	Radio-chemotherapy
rNOE	Relayed nuclear Overhauser effect
T1-w	T1-weighted
T2-w	T2-weighted
TE	Echo time
TR	Repetition time
TSE	Turbo spin echo
WASABI	Simultaneous mapping of water shift and B1
WHO	World Health Organization
Z_{lab}	Label Z-spectrum
Z_{ref}	Reference Z-spectrum

Introduction

Gliomas are the most frequent primary brain tumors in adults. Patient overall survival (OS) is the most objective and relevant measure of meaningful clinical efficacy while the duration of progression-free survival (PFS) commonly serves as surrogate endpoint for OS [1]. Patients with high-grade glioma (HGG, WHO grades III–IV) still face poor prognosis despite gross total resection followed by radio-chemotherapy as therapy of choice [2, 3]. However, HGGs are highly heterogeneous in their therapeutic response due to different radiosensitivity and/or chemosensitivity [4–6]. Unfortunately, stratification of these patients is not possible at diagnosis without histopathological analysis after resection or biopsy. In order to start patient individualized treatment as early as possible, which in turn leads to a better outcome [7], it is of utmost importance to provide noninvasive information about patient prognosis and tumor biology prior to invasive procedures.

To date, contrast-enhanced magnetic resonance imaging (MRI) is one of the key elements in the diagnostic workup of glioma patients [8, 9]. There are many studies reporting OS and PFS association with MRI parameters, particularly based on advanced imaging techniques at 3 T, such as apparent diffusion coefficient (ADC) and relative cerebral blood volume (rCBV) analyses. The majority of these studies found decreased ADC values and increased rCBV values in the tumor region of newly diagnosed or recurrent gliomas associated with worse outcome (OS and/or PFS) [10–15]. However, the results of these various studies are inconsistent in their degree of association, with most approaches being outperformed by clinical parameters, such as patient age, the Karnofsky performance scale (KPS), or molecular characteristics of the tumor [16–18]. In this context, promising results were reported employing deep learning radiomics analyses which combine information extracted from various MR sequences and clinical risk factors [19, 20]. In order to further increase the diagnostic value of these approaches, additional

independent information on the heterogeneous tumor biology is needed.

Chemical exchange saturation transfer (CEST) imaging is a novel MRI technique providing complementary information to current standard MR protocols on the subcellular protein level. Due to its sensitivity to protein concentration [21, 22] and conformation [23–25], as well as intracellular pH [22, 26–28], CEST imaging yields further characterization of the tumor microenvironment. Most of the recently performed CEST studies were conducted using the magnetization transfer ratio asymmetry (MTR_{asym}) technique [29–31]. However, MTR_{asym} approaches have multiple contributions from different CEST effects, including conventional upfield and downfield relayed nuclear Overhauser effect (rNOE) signals, as well as T_1 and T_2 relaxation, and conventional semisolid magnetization [32]. Consequently, an isolation of different CEST signals (particularly APT and rNOE signals) may enhance information value. This has recently been demonstrated to be feasible employing a multi-Lorentzian fit analysis on data with high spectral resolution acquired at 7-T MRI [33].

The purpose of this study was to prospectively investigate the association of relaxation-compensated multi-pool CEST MRI with overall survival and progression-free survival in patients with newly diagnosed, previously untreated high-grade glioma. We hypothesized that the information provided by protein-weighted CEST imaging is linked to patient outcome and survival. To the best of our knowledge, this is the first investigation of the prognostic value of CEST MRI on the survival and progression-free survival of glioma patients.

Materials and methods

Patients

Thirty-one patients with newly diagnosed intra-axial mass lesions were included in this prospective IRB-approved study between January 2014 and September 2017. Written informed consent was obtained from all patients after the nature and possible consequences of the study were explained. Study inclusion criteria were MRI findings suspicious for HGG, previously untreated, age > 18 years, and eligibility for 7-T MRI. In total, 26 patients were histopathologically confirmed with HGG (24 glioblastoma multiforme (GBM) WHO grade IV, 2 anaplastic astrocytoma WHO grade III). Glioma grade was determined based on the 2016 WHO classification of tumors of the central nervous system [34]. Five patients had tumors of a non-glial entity (metastasis, lymphoma); these patients were consequently excluded from the analysis. Patient characteristics of the study cohort are provided in Table 1. The study cohort has previously been reported [32, 35] and a subcohort of 11 patients has been included in the method-based publications [33, 36]. However, no investigations of OS and PFS have previously been performed.

OS was calculated from the date of the MRI examination to death or the date of last inquiry at the registration office where the patient was reported to be alive. PFS was determined as the time from the date of the MRI examination to the date of progression according to the updated RANO criteria [37]. The date of the last inquiry and considered follow-up examination was May 7, 2018. At that time, ten patients were still alive and thus censored in the statistical analysis. One patient had not experienced progression of disease, and from two patients, the PFS could not be determined due to the fact that their follow-up visits took place at outside institutions. These three patients were consequently censored in the PFS analysis.

Clinical MRI at 3 T

The acquisition of conventional MRI exams was performed at 3 T employing the following protocol parameters: T1-weighted gadolinium contrast-enhanced MRI (gdce-T1) (echo time (TE) = 4.04 ms; repetition time (TR) = 1710 ms; field of view (FoV) in mm^2, 256 × 256; matrix, 512 × 512; slice thickness = 1 mm), T2 fluid-attenuated inversion recovery (FLAIR) (TE = 135 ms; TR = 8500 ms; FoV, 230 × 172; matrix, 256 × 192; slice thickness = 5 mm), T2-weighted MRI turbo spin echo (TSE) (TE = 86 ms; TR = 5550 ms; FoV, 229 × 172; matrix, 384 × 230; slice thickness = 5 mm), and diffusion-weighted imaging (DWI) yielding the apparent diffusion coefficient (ADC) (echo planar readout, TE = 90 ms; TR = 5300 ms; $b = 0$ mm^2/s and $b = 1200$ mm^2/s; FoV, 229 × 229; matrix, 130 × 130; slice thickness = 5 mm).

Relaxation-compensated CEST MRI at 7 T

Relaxation-compensated multi-pool CEST MRI was performed on a 7.0-T (297.2 MHz) whole-body MRI scanner (MAGNETOM 7 T; Siemens Healthineers) employing a custom-developed CEST sequence based on a 2-D single-slice gradient echo (GRE) and a single-channel transmit (Tx)/24-channel receive (Rx) 1H head coil, as previously described [32, 36, 38].

To achieve simultaneous, separate quantification of amide and rNOE signals in Z-spectra, voxels were fit pixel-wise by multiple Lorentzian functions [33], resulting in a label (Z_{lab}) and a corresponding reference Z-spectrum (Z_{ref}) for each CEST effect.

The non-relaxation-compensated magnetization transfer Lorentzian difference (MTR_{LD}) of a CEST pool (e.g., APT, rNOE) is given by [21]:

$$MTR_{LD} = Z_{Ref} - Z_{Lab}$$

Table 1 Summary of the patients' characteristics. All diagnoses were histopathologically proven through surgical resection or tumor biopsy after CEST MRI at 7.0 T. *RCT* radio-chemotherapy, *n/a* data not available)

Characteristic		Number	Percentage
Age at diagnosis (years)	Mean 57 ± 14		
Sex	Female	11	42%
	Male	15	58%
Disease	WHO IV	24	92%
	WHO III	2	8%
MGMT promotor methylation	Unmethylated	6	23%
	Methylated	13	50%
	Indeterminate, n/a	7	27%
IDH1-R132H	Wild type	22	85%
	Mutation	3	12%
	n/a	1	4%
Treatment	Debulking surgery + RCT	16	62%
	Biopsy + RCT	10	38%
Overall survival (days) (-05/2018)	Mean 327 ± 137	16	62%
	Alive, n/a	10	38%
Progression-free survival (days)	Mean 249 ± 174	23	88%
(-05/2018)	No progress, n/a	3	12%

Lorentzian difference contrasts were determined for the amide peak at 3.5 ppm (APT_{LD}) and for NOE signals at −3.5 ppm (NOE_{LD}). The MTR_{LD} metric is not relaxation-compensated. Relaxation compensation can be achieved by employing the apparent exchange-dependent relaxation (AREX) [28, 33] metric including MT, T_1, and T_2 relaxation correction of the CEST contrasts:

$$\mathrm{AREX} = \frac{\left(\frac{1}{Z_{\mathrm{Lab}}} - \frac{1}{Z_{\mathrm{Ref}}}\right)}{T_1}$$

This metric was used to calculate the relaxation-compensated APT (APT_{AREX}) and NOE contrast (NOE_{AREX}); the unit of these values is hertz (Hz). Ultimately, downfield rNOE contributions that additionally resonate at 3.5 ppm can be removed by employing the downfield-rNOE-suppressed amide proton transfer (dns-APT/dns-APT_{AREX}) metric [36] with $\Delta\omega = 3.5$ ppm and $r_{\mathrm{rNOE}} = 0.2$:

$$\mathrm{dns{-}APT}(+\Delta\omega) = \mathrm{AREX}(+\Delta\omega) - r_{\mathrm{rNOE}} \cdot \mathrm{AREX}(-\Delta\omega)$$

B_0 and B_1 field inhomogeneities were determined using the water shift and B_1 method (*WASABI*) [39] and reconstructed corresponding to $B_1 = 0.6$-μT saturation amplitude [40]. In the literature, rNOE effects are often referred to as NOE effects. This convention is also followed in this manuscript for better readability.

For data co-registration, a high-resolution T2-w turbo spin echo (TSE) sequence (TE = 54 ms; TR = 14,130 ms; FoV, 220 × 178.8 mm^2; matrix, 512 × 416.3; slice thickness, 2 mm) was additionally acquired at 7 T. Image co-registration was performed using an automatic multi-modal rigid registration algorithm of the Medical Imaging Interaction Toolkit (MITK) [38].

Data analysis and statistics

One region of interest (ROI) was determined in each patient on T2-FLAIR and gdce T1-w images (pre- and post-injection) (Fig. S1). This ROI comprised the peritumoral edema and contrast-enhancing tumor, excluded necrotic tumor areas and blood products thoroughly. Tumor segmentation was performed with the MITK software [41] by a radiologist (R1: A.R.) with more than 10 years of experience in neuroimaging. Furthermore, a second segmentation was performed by another radiologist (R2: H.S., expert with more than 30 years of experience) in order to test for inter-reader agreement using Bland-Altman analyses and intraclass correlation (ICC) analyses. The two radiologists were blinded to each other's segmentations.

Univariate Cox regression analyses were performed for OS and PFS with the following variables: MRI parameters: APT_{LD}, APT_{AREX}, dns-APT_{AREX}, NOE_{LD}, NOE_{AREX}, and ADC; clinical parameters: age, gender, MGMT promotor methylation status, and treatment: debulking surgery + radio-chemotherapy (RCT) versus biopsy + RCT. Hazard ratios and corresponding 95% confidence intervals were calculated. A possible association of IDH1-R132H mutation status and OS/PFS was not assessed, since only three patients of the study cohort were confirmed to have an IDH mutation. The Kaplan-Meier method with univariate two-sided log-rank

statistics was additionally performed for MRI parameters which were significantly associated with OS and/or PFS after dichotomization into two groups at the median.

Furthermore, possible interdependence of available clinical parameters and all MRI parameters were assessed. For continuous variables, Spearman rank-order correlation analyses were performed while Mann-Whitney rank sum tests were applied to dichotomized data. For statistical analyses, the level of significance was set to $p < 0.05$. All statistical analyses were performed with R (Version 3.5.1).

Subgroup analysis: glioblastoma IDH wild-type patients

It was recently shown that relaxation-compensated CEST MRI, particularly APT_{AREX} and dns-APT_{AREX} imaging, is strongly associated with IDH mutation status [32]. Therefore, the subcohort of histopathologically confirmed glioblastoma IDH wild-type (IDH-wt) patients (Table 1, $n = 22$) was additionally assessed regarding possible associations of CEST MRI and patient OS/PFS using univariate Cox regression analyses to exclude possible bias from IDH mutation status in the study cohort.

Results

General imaging characteristics of CEST MRI

Increased amide signals from relaxation-compensated CEST MRI (APT_{AREX}, dns-APT_{AREX}) were observed in the tumor area, especially in regions adjacent to blood-brain barrier disruption and partially overlapping with the gadolinium contrast enhancement. Hyperintense APT signals were also observed in regions with decreased ADC values (Fig. 1). APT effects tended to be more pronounced in patients with shorter OS and/or PFS. Figure 1 depicts two representative patients of the study cohort for the relaxation-compensated APT metrics with (i) relatively long OS + PFS and (ii) relatively short OS + PFS, respectively. Hyperintense amide signals in the tumor region delineate more clearly on the dns-APT contrast compared with the APT_{AREX} contrast due to the additional suppression of downfield resonating NOE effects. NOE-mediated effects (NOE_{LD} and NOE_{AREX}) were decreased in the tumor area (including necrosis, contrast enhancement, and large parts of the peritumoral edema) in all patients of the study cohort.

Overall survival

Mean overall survival was 327 ± 137 days and 10 patients were still alive at the end of the study and, thus, censored in the statistical analysis. Among the tested clinical parameters, patient age (HR = 1.10, $p = 0.001$) and therapy (biopsy + RCT versus debulking surgery + RCT; HR = 3.68, $p = 0.03$) were significant for OS in the univariate Cox regression analysis (Table 2A). Here, patients who were younger and underwent full therapy (debulking surgery + adjuvant RCT) had a better clinical outcome. Regarding gender and MGMT status, a tendency toward shorter survival was observed for males (HR = 2.76, $p = 0.08$) and patients with unmethylated MGMT promotor (HR = 2.62, $p = 0.12$). Univariate Cox regression of the investigated MRI metrics yielded significant association of patient OS with the relaxation-compensated CEST contrasts APT_{AREX} (HR = 3.15, $p = 0.02$), dns-APT_{AREX} (HR = 2.51, $p = 0.03$), and NOE_{AREX} (HR = 1.40, $p = 0.01$) (Table 2A).

Kaplan-Meier analysis of survival was significant for APT_{AREX} after data dichotomization at the median ($p = 0.009$) (Fig. 2). Survival times of HGG patients with tumor signal intensities less or equal to median ($APT_{AREX} \leq 4.23\%$) were significantly increased (mean 376 ± 170 days, median 411 days) compared with patients with signal intensities above the median ($APT_{AREX} > 4.23\%$; mean 289 ± 110 days, median 292 days). Kaplan-Meier statistics were not significant for the other MRI parameters ($p > 0.05$). A tendency toward longer survival was however also observed for the dns-APT metric ($p = 0.25$) (Fig. 2A, B).

Progression-free survival

Mean overall progression-free survival was 249 ± 174 days and 3 patients had not yet experienced disease progression (or the follow-up data was not available) and were, thus, censored in the statistical analysis. In the univariate Cox regression analyses, patient age (HR = 1.04, $p = 0.048$) was the only significant clinical parameter (Table 2A). A tendency toward longer PFS was observed for therapy (debulking surgery + RCT versus biopsy + RCT, $p = 0.08$).

Among the investigated MRI parameters, both relaxation-compensated APT metrics (APT_{AREX}, dns-APT_{AREX}) and the APT_{LD} contrast were significant for PFS (HR = 1.83, $p = 0.009$; HR = 2.61, $p = 0.002$; and HR = 1.46, $p = 0.042$). Furthermore, DWI-derived ADC values tended to be lower in patients with shorter PFS (HR = 2.23, $p = 0.052$). All results of the univariate Cox regression analyses are summarized in Table 2A.

Kaplan-Meier analyses of PFS were significant for APT_{AREX} and dns-APT_{AREX} after data dichotomization at the median ($p = 0.005$ and $p = 0.004$) (Fig. 2C, D) but not significant for the other MRI parameters ($p > 0.05$). HGG patients with APT_{AREX} signal intensities less than or equal to the median ($APT_{AREX} \leq 4.23$ %) had significantly longer PFS (mean 334 ± 185 days, median 287 days) compared with patients with intensities greater than the median (APT_{AREX} > 4.23%; mean 140 ± 60 days, median 124 days). The strongest association with PFS was found for the dns-APT_{AREX} contrast with a significantly increased PFS in patients with signal intensities less than or equal to the median

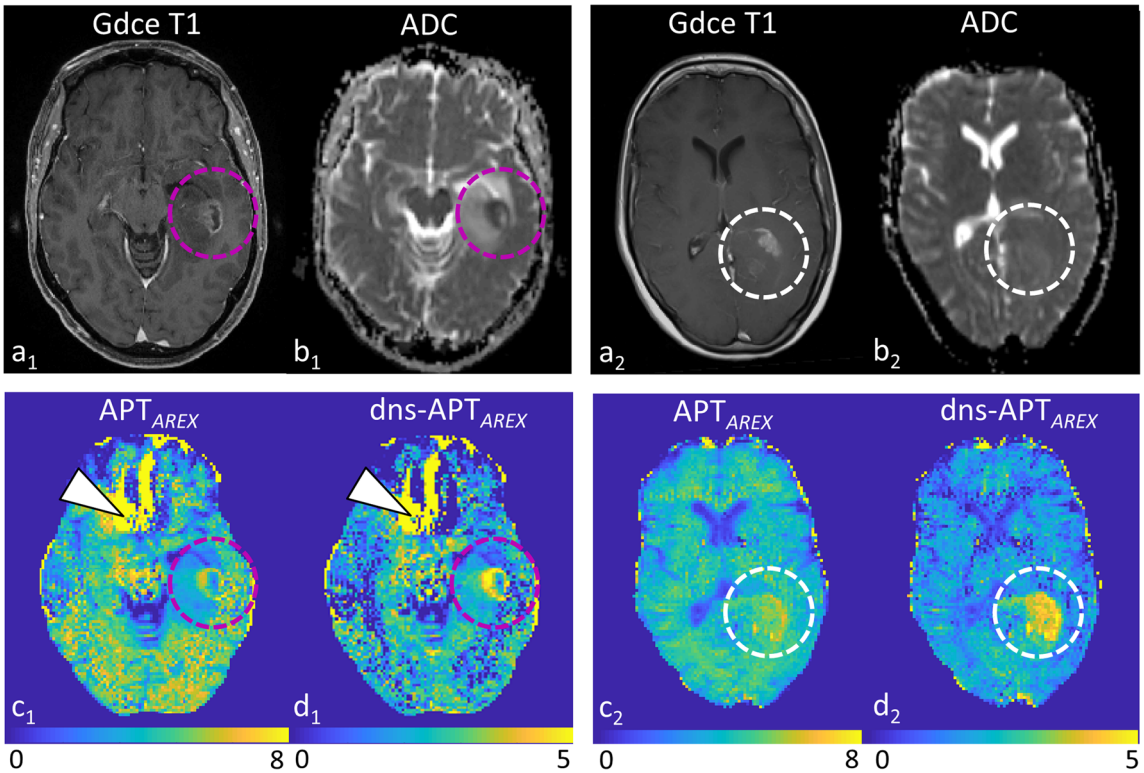

Fig. 1 Relaxation-compensated APT MRI in HGG patients at 7.0 T. Two representative glioblastoma patients of the study cohort are shown. One 51-year-old patient ($\mathbf{a}_1$–$\mathbf{d}_1$) with a relatively long period of PFS (279 days) and an OS of 479 days and a 44-year-old patient ($\mathbf{a}_2$–$\mathbf{d}_2$) with a relatively short period of PFS (90 days) and an OS of 352 days. Increased amide signals (c_i: APT_{AREX}, d_i: dns-APT_{AREX}) can be observed in the tumor area of both patients, especially adjacent to blood-brain barrier disruption and overlapping with the gadolinium contrast enhancement. APT effects are, however, more pronounced in the patient with shorter PFS and OS ($\mathbf{c}_2$–$\mathbf{d}_2$) particularly at dns-APT imaging ($\mathbf{d}_2$). In the patient with longer OS and PFS ($\mathbf{a}_1$–$\mathbf{d}_1$), the APT hyperintensity ($\mathbf{c}_1$–$\mathbf{d}_1$) matches very well the hypointense signal alterations on the ADC map ($\mathbf{b}_1$), possibly indicating areas with increased cellularity. In the patient with the worse outcome ($\mathbf{a}_1$–$\mathbf{d}_1$), no clear ADC hypointensity displays in the tumor region ($\mathbf{b}_2$), while amide signals are markedly increased ($\mathbf{c}_2$–$\mathbf{d}_2$). Signal artifacts of the nasal sinuses are indicated (white arrow heads) (AREX CEST signal intensities (c_i–d_i) in % Hz)

(dns-$APT_{AREX} \leq 2.27\%$; mean 344 ± 189 days, median 297 days) compared with patients with intensities greater than the median (dns-$APT_{AREX} > 2.27\%$; mean 147 ± 62 days, median 130 days).

Inter-reader agreement and interdependence of MRI and clinical parameters

Bland-Altman analyses of the investigated MRI contrasts measured by the two radiologists (R1, R2) showed high concordance (Fig. S2). The large majority of values (96.15%) lied within the 95% limits of agreement for all MRI contrasts. Moreover, ICC statistics indicated high correlations between the two different segmentations (Table S1, ICC range 0.98–0.99, 95% CI 0.95–1.00). All HRs and corresponding p values of the univariate Cox regression analysis agreed very well between both readers (Table 2, Table S2). The only discrepancy was that the expert's segmentation (R2) yielded an additional significant association of NOE_{AREX} and ADC with PFS ($p = 0.048$ and $p = 0.032$) compared with the other reading ($p = 0.058$ and $p = 0.052$).

Spearman rank correlation analysis did not show significant interdependence of patient age and any MRI contrast ($p > 0.05$). Furthermore, MGMT promotor methylation status and type of therapy did not show significant association with the tested MRI parameters ($p > 0.05$). Gender was not associated with any APT contrast ($p > 0.05$) but statistically significant for the NOE_{LD} ($p = 0.007$) and NOE_{AREX} (0.004) metrics. NOE-mediated signal intensities were significantly increased in tumors of males (NOE_{AREX}: median = 10.40%, IQR = 5.02–9.89%; NOE_{LD}: median = 11.30%, IQR = 10.60–12.50%) compared with females (NOE_{AREX}: median = 10.40%, IQR = 5.02–9.89%; NOE_{LD}: median = 10.30%, IQR = 6.25–11.10%).

Subgroup analysis: glioblastoma IDH wild-type patients

Due to the known association of CEST MRI and IDH mutation status in glioma [32, 42], univariate Cox analysis was additionally performed for the investigated MRI metrics and clinical parameters in the homogenous subcohort of glioblastoma IDH wild-type (IDH-wt) patients ($n = 22$). The APT_{AREX} contrast was significantly associated with patient OS (HR = 3.25, p =

Table 2 Univariate Cox proportional hazards analyses for all tested regressors. Analyses were performed for the whole study cohort (A: $n = 26$ HGG patients) and a homogenous subcohort of glioblastoma IDH-wt patients (B: $n = 22$). *HR* hazard ratio, *CI* confidence interval, *m* male, *f* female. MGMT status: *met* methylated promotor, *unm* unmethylated promotor. Therapy: *RCT* definitive radio-chemotherapy, *DSRCT* debulking surgery plus RCT

Regressor	Overall survival		Progression-free survival	
	HR (95% CI)	*p* value	HR (95% CI)	*p* value
A) Study cohort: high-grade glioma patients ($n = 26$)				
MRI contrasts				
NOE_{LD}	1.30 (0.98–1.73)	0.065	1.11 (0.96–1.29)	0.165
NOE_{AREX}	1.40 (1.07–1.83)	0.014*	1.16 (0.99–1.35)	0.058
APT_{LD}	1.46 (0.95–2.26)	0.085	1.46 (1.01–2.01)	0.042*
APT_{AREX}	3.15 (1.22–8.16)	0.018*	1.83 (1.16–2.89)	0.009**
dns-APT_{AREX}	2.51 (1.13–5.60)	0.025*	2.61 (1.42–4.83)	0.002**
ADC	0.78 (0.57–1.09)	0.143	0.80 (0.63–1.00)	0.052
Clinical parameter				
Age (years)	1.10 (1.04–1.17)	0.001**	1.04 (1.00–1.08)	0.048*
Gender (m vs. f)	2.76 (0.88–8.67)	0.081	1.09 (0.47–2.55)	0.826
MGMT status (unm vs. met)	2.62 (0.76–8.98)	0.126	2.22 (0.68–7.25)	0.189
Therapy (RCT vs. DSRCT)	3.68 (1.17–11.57)	0.026*	2.23 (0.91–5.46)	0.080
B) Subcohort: glioblastoma IDH wild-type patients ($n = 22$)				
MRI contrasts				
NOE_{LD}	1.10 (0.71–1.69)	0.681	0.96 (0.66–1.42)	0.854
NOE_{AREX}	1.24 (0.90–1.71)	0.196	0.94 (0.68–1.29)	0.701
APT_{LD}	1.15 (0.58–2.28)	0.699	1.94 (0.93–4.04)	0.078
APT_{AREX}	3.25 (1.03–10.26)	0.044*	1.82 (0.87–3.80)	0.112
dns-APT_{AREX}	2.15 (0.69–6.68)	0.184	2.42 (1.03–5.68)	0.042*
ADC	0.96 (0.63–1.47)	0.867	0.87 (0.66–1.15)	0.327
Clinical parameter				
Age (years)	1.10 (1.03–1.18)	0.007**	1.02 (0.97–1.07)	0.383
Gender (m vs. f)	1.51 (0.48–4.79)	0.481	0.71 (0.28–1.81)	0.469
MGMT status (unm vs. met)	2.05 (0.60–6.98)	0.253	1.59 (0.49–5.15)	0.437
Therapy (RCT vs. DSRCT)	4.02 (1.21–13.33)	0.023*	1.91 (0.73–4.95)	0.185

Level of significance: *$p < 0.05$, **$p < 0.01$

0.04), while the dns-APT metric was significantly associated with PFS (HR = 2.42, $p = 0.04$). In contrast to the entire study cohort, no significant associations of OS or PFS were found for the NOE_{AREX} or APT_{LD} metric ($p > 0.05$).

Among the tested clinical parameters, patient age (HR = 1.10, $p < 0.01$) and therapy (HR = 4.02, $p = 0.02$) were significant for OS, while no significant association was found for PFS ($p > 0.05$). The results of the glioblastoma IDH-wt subcohort analysis are summarized in Table 2B.

Discussion

In this work, we have shown that relaxation-compensated amide proton transfer MRI signal intensity at 7.0 T is associated with overall survival and progression-free survival in newly diagnosed, previously untreated glioma patients. Therefore, the study adds an important element to the fast-growing body of evidence regarding the prognostic value of CEST MRI in neuro-oncology.

The current study showed that glioma patients with increased APT values were more likely to progress sooner and live shorter, respectively. This effect may be caused by strong alterations of amino acid concentrations and global upregulation of protein expression in more aggressive brain tumors. Our findings were particularly conclusive for the relaxation-compensated APT_{AREX} and dns-APT_{AREX} contrasts which showed a significant association between increased amide signals and patient outcome for OS and PFS, both for the entire study cohort of HGG patients as well as the GBM IDH-wt subcohort analysis. The dns-APT metric (which additionally removes downfield resonating rNOE effects from the APT_{AREX} contrast) showed the strongest association of all investigated parameters with PFS. The surrogate endpoint PFS is, however, less objective than OS due to the vagueness of patient treatment response evaluation in the early follow-up. The APT_{LD} metric, which is not relaxation-compensated,

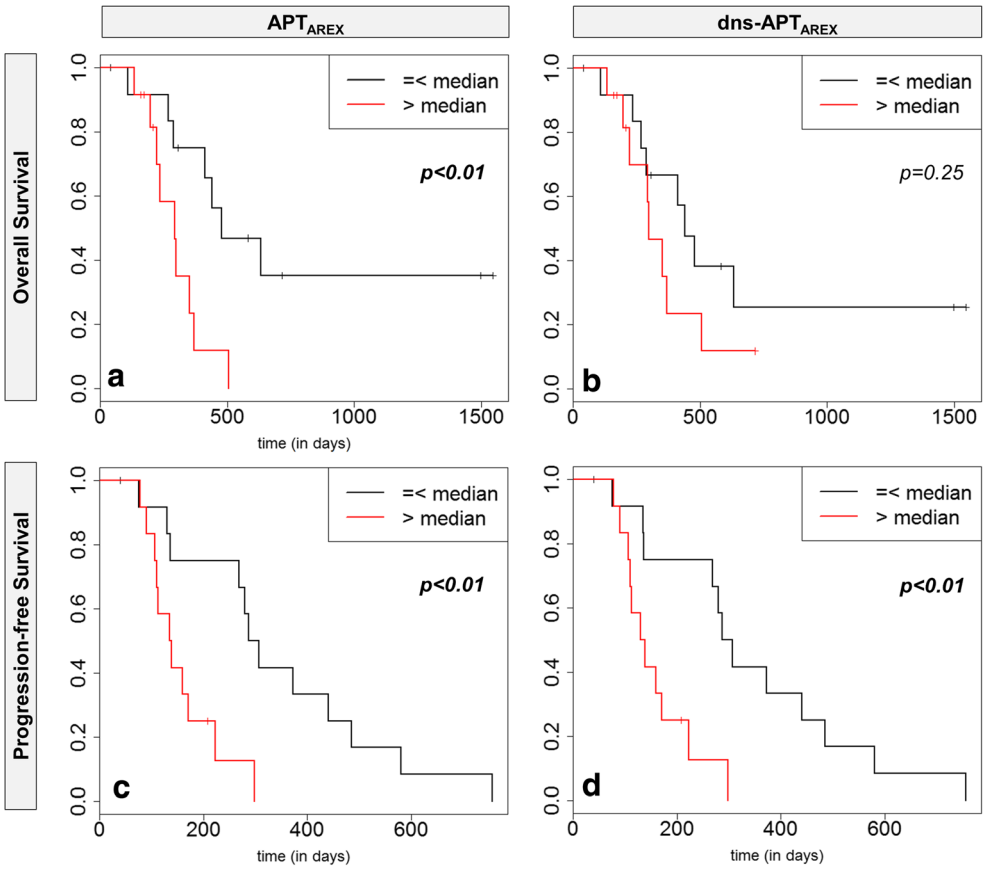

Fig. 2 Kaplan-Meier analysis and log-rank statistics for overall survival (OS: A, B) and progression-free survival (PFS: C, D) after data dichotomization at the median. Significant association with patient OS was found for the relaxation-compensated APT_{AREX} contrast (A, $p = 0.009$), while a tendency toward longer survival was, however, also observed for the dns-APT metric (B, $p = 0.25$). Significant association with PFS was found for both relaxation-compensated APT metrics (C: APT_{AREX}, $p = 0.005$; dns-APT_{AREX}, $p = 0.004$)

was also significant for PFS over all HGG patients. In the subcohort analysis of GBM IDH-wt patients, this association was not observed. The known influence of IDH1 mutation status on the CEST contrasts [32, 42] may explain this finding, since the presence of IDH1 mutation also strongly affects patient outcome [4]. Likewise, the NOE-mediated CEST contrasts were not associated with OS or PFS in the GBM IDH-wt subcohort, while a significant association was found between OS (and PFS, R2) and NOE_{AREX} in the HGG study cohort. Furthermore, underlying MT, T_1, and T_2 relaxation may additionally mask a possible association of the MTR_{LD} metrics and OS or PFS. Therefore, the significant associations of the relaxation-compensated APT contrasts with both OS (APT_{AREX}) and PFS (dns-APT_{AREX}) in the GBM IDH-wt subgroup strongly support the hypothesis that CEST MRI is a predictive biomarker of outcome in glioma patients. In a heterogeneous study cohort of IDH-wt and IDH-mut patients, this association becomes even more evident due to the superimposition of both effects.

Inter-reader agreement analyses showed excellent agreement between the two radiologists. The additionally found significant association of NOE_{AREX} and ADC with PFS for R2 (expert reading) is most likely due to minor deviations between the two different segmentations yielding p values slightly above (R1: $p = 0.058$ and $p = 0.052$) and slightly below (R2: $p = 0.048$ and $p = 0.032$) the alpha level of statistical significance in the univariate Cox analysis.

NOE contrasts generally seem to provide clinically relevant information substantially different from APT-mediated CEST MRI. This is plausible since the underlying mechanism is fundamentally different. Relayed NOE effects are based on dipole-dipole couplings in macro-molecules, proteins, and peptides while amide proton transfer happens via direct exchange of water-bound protons with amide groups [21, 43]. Previous publications showed that NOE signals may enable baseline prediction of therapy response and assessment of early treatment effects in patients with glioma [35] and brain metastases [44] and may correlate with tumor cellularity [45]. In this study cohort, we also found a significant association between NOE signals in tumors (NOE_{LD} and NOE_{AREX}) and gender. To the best of our knowledge, this has not been previously reported but may just be a coincidental finding. This result should, however, be investigated in future studies, on both patients and healthy subjects.

In accordance with the literature, tumor ADC values tended to be decreased in patients with shorter OS and/or PFS in this study [10, 12, 13, 15]. Furthermore, investigated clinical parameters were significantly associated with OS (patient age and therapy) and PFS (therapy). In this context, Burth et al reported for a relatively large retrospective study cohort that parameters derived from conventional clinical MRI scans (e.g., ADC,

rCBV) were generally outperformed by clinical risk factors such as patient age and KPS in a multivariate regression analysis [17]. Clinical scores, however, suffer from the rater's subjectivity. At this point, quantitative non-invasive multiparametric MRI techniques may improve the diagnostic performance of outcome prediction. Our results suggest that relaxation-compensated APT imaging may hereby add valuable information on a subcellular protein level to conventional MRI protocols.

CEST MRI has recently been applied as an imaging biomarker to assess different histologic and genetic subtypes of glioma patients, both at clinical and ultra-high (7 T) field strength. Thereby, several studies showed differentiability of HGG and low-grade gliomas employing APT-w MRI both at 3-T and 7-T MRI [31, 32, 46, 47] and an association of CEST MRI and IDH mutation status as discussed previously in the text [32, 42]. Regarding MGMT promotor methylation status, Jiang et al reported significantly increased APT-w signals in glioblastomas with unmethylated MGMT promotor [48], while no significant differences were found by Paech et al [32]. In summary, these studies strongly suggest that CEST MRI is able to provide non-invasive insights into tumor biology which may in turn help to furthering our understanding of highly heterogeneous and complex gliomas.

Our findings need to be validated in independent, larger study cohorts and at clinical field strength. Recently, several studies reported successful separation of different CEST pools at 3.0 T which may enable immediate applicability of the presented approach in the clinical setting [49, 50]. Our results may motivate and justify such studies.

Some limitations of this work need to be acknowledged. (i) The relatively small size of the study cohort ($n = 26$) is a limitation. However, statistically meaningful results were obtained and the shown data represent the first prospective survival analysis employing CEST MRI. Moreover, these results still stand for the relaxation-compensated APT contrasts in a homogenous subcohort of $n = 22$ GBM IDH-wt patients. (ii) In this work, univariate Cox regression analyses were performed. More sophisticated multivariate regression analyses, however, require larger study cohorts to obtain meaningful results and should, therefore, be addressed in future investigations. (iii) Another possible limitation is the inclusion of patients with different surgical approaches. However, this study cohort represents a common clinical spectrum, which seemingly did not impede the significance of CEST MRI. (iv) Ultimately, B_1 saturation power is known to affect individual CEST effects differently. Consequently, the presented results are only valid for the specific field strength pair (B_0, B_1) = (7 T, 0.6 μT).

Conclusion

Relaxation-compensated APT MRI signal intensity was shown to be associated with OS and PFS in a study cohort of newly diagnosed glioma patients and may therefore enhance the prognostic value of these non-invasive MRI tools at the time of initial diagnosis and during follow-up. Patients with increased APT values were more likely to progress sooner and live shorter, possibly reflecting strong alterations of amino acid concentrations and global upregulation of protein expression in more aggressive brain tumors.

Acknowledgements The authors would like to thank Prof. Dr. Annette Kopp-Schneider for her invaluable help with the statistical analyses and Joseph Weygand, M.S., for carefully proof reading and reviewing of the manuscript.

Funding The authors state that this work has not received any funding.

Compliance with ethical standards

Guarantor The scientific guarantor of this publication is Dr. Daniel Paech.

Conflict of interest The authors of this manuscript declare no relationships with any companies, whose products or services may be related to the subject matter of the article.

Statistics and biometry Prof. Dr. Annette Kopp-Schneider (Division of Biostatistics, German Cancer Research Center, Heidelberg, Germany) kindly provided statistical advice for this manuscript.

Informed consent Written informed consent was obtained from all subjects (patients) in this study.

Ethical approval Institutional Review Board approval was obtained.

Study subjects or cohorts overlap The study cohort has previously been reported (Paech et al. Neuro Oncol, 2018, noy073 and Regnery et al. Oncotarget, 2018, 9:28772–28783) and a subcohort of eleven patients has been included in methodical publications (Zaiss et al. Neuroimage, 2015, 112:180–188 and Zaiss et al. MRM, 2017, 77(1):196–208). However, no investigations of overall survival and progression-free survival have previously been performed.

Methodology
- prospective
- diagnostic or prognostic
- performed at one institution

References

1. Kim KB (2014) PFS as a surrogate for overall survival in metastatic melanoma. Lancet Oncol 15:246–248
2. Porter KR, McCarthy BJ, Freels S, Kim Y, Davis FG (2010) Prevalence estimates for primary brain tumors in the United States by age, gender, behavior, and histology. Neuro Oncol 12:520–527
3. Stupp R, Roila F (2009) Malignant glioma: ESMO clinical recommendations for diagnosis, treatment and follow-up. Ann Oncol 20(Suppl 4):126–128

4. Yan H, Parsons DW, Jin G et al (2009) IDH1 and IDH2 mutations in gliomas. N Engl J Med 360:765–773
5. Hegi ME, Diserens AC, Gorlia T et al (2005) MGMT gene silencing and benefit from temozolomide in glioblastoma. N Engl J Med 352:997–1003
6. Wen PY, Kesari S (2008) Malignant gliomas in adults. N Engl J Med 359:492–507
7. Cerqua R, Balestrini S, Perozzi C et al (2016) Diagnostic delay and prognosis in primary central nervous system lymphoma compared with glioblastoma multiforme. Neurol Sci 37:23–29
8. Henson JW, Gaviani P, Gonzalez RG (2005) MRI in treatment of adult gliomas. Lancet Oncol 6:167–175
9. Ellingson BM, Chung C, Pope WB, Boxerman JL, Kaufmann TJ (2017) Pseudoprogression, radionecrosis, inflammation or true tumor progression? Challenges associated with glioblastoma response assessment in an evolving therapeutic landscape. J Neurooncol 134(3):495–504
10. Pope WB, Qiao XJ, Kim HJ et al (2012) Apparent diffusion coefficient histogram analysis stratifies progression-free and overall survival in patients with recurrent GBM treated with bevacizumab: a multi-center study. J Neurooncol 108:491–498
11. Oh J, Henry RG, Pirzkall A et al (2004) Survival analysis in patients with glioblastoma multiforme: predictive value of choline-to-n-acetylaspartate index, apparent diffusion coefficient, and relative cerebral blood volume. J Magn Reson Imaging 19:546–554
12. Ellingson BM, Cloughesy TF, Lai A et al (2011) Graded functional diffusion map–defined characteristics of apparent diffusion coefficients predict overall survival in recurrent glioblastoma treated with bevacizumab. Neuro Oncol 13:1151–1161
13. Higano S, Yun X, Kumabe T et al (2006) Malignant astrocytic tumors: clinical importance of apparent diffusion coefficient in prediction of grade and prognosis. Radiology 241:839–846
14. Law M, Young RJ, Babb JS et al (2008) Gliomas: predicting time to progression or survival with cerebral blood volume measurements at dynamic susceptibility-weighted contrast-enhanced perfusion MR imaging. Radiology 247:490–498
15. Hamstra DA, Chenevert TL, Moffat BA et al (2005) Evaluation of the functional diffusion map as an early biomarker of time-to-progression and overall survival in high-grade glioma. Proc Natl Acad Sci U S A 102:16759–16764
16. Bonekamp D, Deike K, Wiestler B et al (2015) Association of overall survival in patients with newly diagnosed glioblastoma with contrast-enhanced perfusion MRI: comparison of intraindividually matched T1 - and T2 (*) -based bolus techniques. J Magn Reson Imaging 42:87–96
17. Burth S, Kickingereder P, Eidel O et al (2016) Clinical parameters outweigh diffusion- and perfusion-derived MRI parameters in predicting survival in newly diagnosed glioblastoma. Neuro Oncol 18:1673–1679
18. Wiestler B, Kluge A, Lukas M et al (2016) Multiparametric MRI-based differentiation of WHO grade II/III glioma and WHO grade IV glioblastoma. Sci Rep 6:35142
19. Kickingereder P, Götz M, Muschelli J et al (2016) Large-scale radiomic profiling of recurrent glioblastoma identifies an imaging predictor for stratifying anti-angiogenic treatment response. Clin Cancer Res 22:5765–5771
20. Lao J, Chen Y, Li ZC et al (2017) A deep learning-based radiomics model for prediction of survival in glioblastoma multiforme. Sci Rep 7:10353
21. Jones CK, Huang A, Xu J et al (2013) Nuclear Overhauser enhancement (NOE) imaging in the human brain at 7T. Neuroimage 77:114–124
22. Jin T, Wang P, Zong X, Kim SG (2013) MR imaging of the amide-proton transfer effect and the pH-insensitive nuclear overhauser effect at 9.4 T. Magn Reson Med 69:760–770
23. Zaiss M, Kunz P, Goerke S, Radbruch A, Bachert P (2013) MR imaging of protein folding in vitro employing nuclear-Overhauser-mediated saturation transfer. NMR Biomed 26:1815–1822
24. Goerke S, Zaiss M, Kunz P et al (2015) Signature of protein unfolding in chemical exchange saturation transfer imaging. NMR Biomed 28:906–913
25. Longo DL, Di Gregorio E, Abategiovanni R et al (2014) Chemical exchange saturation transfer (CEST): an efficient tool for detecting molecular information on proteins' behaviour. Analyst 139:2687–2690
26. Zhou J, Payen JF, Wilson DA, Traystman RJ, van Zijl PC (2003) Using the amide proton signals of intracellular proteins and peptides to detect pH effects in MRI. Nat Med 9:1085–1090
27. Sun PZ, Benner T, Copen WA, Sorensen AG (2010) Early experience of translating pH-weighted MRI to image human subjects at 3 Tesla. Stroke 41:S147–S151
28. Zaiss M, Xu J, Goerke S et al (2014) Inverse Z-spectrum analysis for spillover-, MT-, and T1-corrected steady-state pulsed CEST-MRI–application to pH-weighted MRI of acute stroke. NMR Biomed 27:240–252
29. Zhou J, Lal B, Wilson DA, Laterra J, van Zijl PC (2003) Amide proton transfer (APT) contrast for imaging of brain tumors. Magn Reson Med 50:1120–1126
30. Zhou J, Blakeley JO, Hua J et al (2008) Practical data acquisition method for human brain tumor amide proton transfer (APT) imaging. Magn Reson Med 60:842–849
31. Togao O, Yoshiura T, Keupp J et al (2014) Amide proton transfer imaging of adult diffuse gliomas: correlation with histopathological grades. Neuro Oncol 16:441–448
32. Paech D, Windschuh J, Oberhollenzer J et al (2018) Assessing the predictability of IDH mutation and MGMT methylation status in glioma patients using relaxation-compensated multi-pool CEST MRI at 7.0 Tesla. Neuro Oncol 20(12):1661–1671
33. Zaiss M, Windschuh J, Paech D et al (2015) Relaxation-compensated CEST-MRI of the human brain at 7 T: unbiased insight into NOE and amide signal changes in human glioblastoma. Neuroimage 112:180–188
34. Louis DN, Perry A, Reifenberger G et al (2016) The 2016 World Health Organization Classification of Tumors of the Central Nervous System: a summary. Acta Neuropathol 131:803–820
35. Regnery S, Adeberg S, Dreher C et al (2018) Chemical exchange saturation transfer MRI serves as predictor of early progression in glioblastoma patients. Oncotarget 9:28772–28783
36. Zaiss M, Windschuh J, Goerke S et al (2017) Downfield-NOE-suppressed amide-CEST-MRI at 7 Tesla provides a unique contrast in human glioblastoma. Magn Reson Med 77:196–208
37. Wen PY, Macdonald DR, Reardon DA et al (2010) Updated response assessment criteria for high-grade gliomas: response assessment in neuro-oncology working group. J Clin Oncol 28:1963–1972
38. Zaiss M, Zu Z, Xu J et al (2015) A combined analytical solution for chemical exchange saturation transfer and semi-solid magnetization transfer. NMR Biomed 28:217–230
39. Schuenke P, Windschuh J, Roeloffs V, Ladd ME, Bachert P, Zaiss M (2017) Simultaneous mapping of water shift and B1 (WASABI)—application to field-inhomogeneity correction of CESTMRI data. Magn Reson Med 77:571–580
40. Windschuh J, Zaiss M, Meissner JE et al (2015) Correction of B1-inhomogeneities for relaxation-compensated CEST imaging at 7 T. NMR Biomed 28:529–537
41. Nolden M, Zelzer S, Seitel A et al (2013) The Medical Imaging Interaction Toolkit: challenges and advances: 10 years of open-source development. Int J Comput Assist Radiol Surg 8:607–620
42. Shanshan J, Tianyu Z, Eberhart GC et al (2017) Predicting IDH mutation status in grade II gliomas using amide proton transfer-weighted (APTw) MRI. Magn Reson Med 78:1100–1109

43. Paech D, Zaiss M, Meissner JE et al (2014) Nuclear Overhauser enhancement mediated chemical exchange saturation transfer imaging at 7 tesla in glioblastoma patients. PLoS One 9:e104181
44. Desmond KL, Mehrabian H, Chavez S et al (2017) Chemical exchange saturation transfer for predicting response to stereotactic radiosurgery in human brain metastasis. Magn Reson Med 78: 1110–1120
45. Paech D, Burth S, Windschuh J et al (2015) Nuclear Overhauser enhancement imaging of glioblastoma at 7 Tesla: region specific correlation with apparent diffusion coefficient and histology. PLoS One 10:e0121220
46. Choi YS, Ahn SS, Lee SK et al (2017) Amide proton transfer imaging to discriminate between low- and high-grade gliomas: added value to apparent diffusion coefficient and relative cerebral blood volume. Eur Radiol 27:3181–3189
47. Sakata A, Okada T, Yamamoto A et al (2015) Grading glial tumors with amide proton transfer MR imaging: different analytical approaches. J Neurooncol 122:339–348
48. Jiang S, Rui Q, Wang Y et al (2017) Discriminating MGMT promoter methylation status in patients with glioblastoma employing amide proton transfer-weighted MRI metrics. Eur Radiol 28(5): 2115–2123
49. Heo H-Y, Zhang Y, Jiang S, Lee DH, Zhou J (2016) Quantitative assessment of amide proton transfer (APT) and nuclear overhauser enhancement (NOE) imaging with extrapolated semisolid magnetization transfer reference (EMR) signals: II. Comparison of three EMR models and application to human brain glioma at 3 Tesla. Magn Reson Med 75:1630–1639
50. Xu J, Yadav NN, Bar-Shir A et al (2014) Variable delay multi-pulse train for fast chemical exchange saturation transfer and relayed-nuclear overhauser enhancement MRI. Magn Reson Med 71: 1798–1812